

Development of electrochemical sensor based on aptamer specific to lung cancer tumor marker

A Shabalina¹, D Sharko^{1,2}, L Matushina^{1,2}, D Ezhov¹

¹Laboratory of Advanced Materials and Technologies, *Siberian Physical-Technical Institute of Tomsk State University*, 1 Novosobornaya Square, Tomsk 634050, Russian Federation

²Chemical Department, *Tomsk State University*, 36 Lenina Avenue, Tomsk 634050, Russian Federation

¹E-mail: shabalinaav@gmail.com

Abstract. Electrochemical aptasensor is a sensor based on an indicator electrode covered with a layer of an aptamer that is able to bind target molecules with high specificity. In this work, DNA-aptamer LC-2108 specific to lung cancer tumor marker was immobilized onto the surface of golden screen-printed and disc electrodes. The electrodes were studied by conventional electrochemical methods—cyclic voltammetry and electrochemical impedance spectroscopy. The current increase and electron transfer resistance decrease were registered. It seems as if the aptamer presence facilitated the electron transfer through the electrode-solution boundary. As the possible reasons of such an unusual electrochemical behavior we proposed the unordinary or irregular structure of the aptamer layer on the Au surface or the specific electrochemical properties of the aptamer itself.

1. Introduction

Biosensor is a sensor consisted of a biological component and a detecting part. Any suitable physical, chemical, or physical-chemical detector can be used for signal obtaining. But, the biological part used for recognition and/or binding of the target molecules has to meet a list of requirements [1]. Firstly, it must bind or recognize target molecules. Under interaction with the target, the biosensing element must produce effect measurable by the detector. It must exhibit high selectivity to the target analyte. In addition, the biological component has to be stable, cost-effective, reusable, etc. Among the most widely used biosensing elements, there are enzymes, antibodies, and aptamers. Aptamers exhibit a number of advantages. The most important one is the chemical way of their synthesis, i.e. aptamer specific to a certain target can be synthesized using known technology [2]. Aptamers are also stable under conditions that are normally extreme for biomedical objects (aptamers can be used in more aggressive solutions and temperatures than that are normal for the human organism). Moreover, the sensors based on aptamers (aptasensors) can be used more than for one analysis, i.e. they are reusable.

Electrochemical aptasensors are based on indicator electrodes covered with an aptamer. Golden electrode is the most often indicator electrode used for the aptasensors development. Aptamers can be attached to the electrode surface through the Au-S bond (aptamer normally contains the thiolate linker on its end). Then the aptasensor is immersed into a solution of a redox mediator—a substance that is able to oxidize and reduce on the electrode surface giving a signal (peak of current on voltammogram, for example). An aptamer being an organic molecule with a certain size normally hinder the redox



mediator molecules transport to the electrode surface and the signal decreases. Under binding the specific target, the blocking layer on the electrode surface becomes thicker and the signal further decreases [3].

Thus, the most important factors affecting the aptasensor effectiveness are the following: aptamer layer thickness, its regularity, and stability including the stability during electrochemical measurements. When a new aptasensor is developed, this is an important task to obtain a high qualitative layer of aptamer on the electrode surface and to characterize this layer using different methods. In this work, we dealt with the aptamer specific to the lung cancer tumor marker. The tumor marker and the DNA-aptamer to it (LC-2108) were proposed by the research group of A.S. Kichkailo from Krasnoyarsk State Medical University named after prof. V.F. Voino-Yasenetsky (Krasnoyarsk, Russia) [4]. To characterize aptamer layer on the electrode surface we used standard electrochemical methods—cyclic voltammetry (CV) and electrochemical impedance spectroscopy (EIS).

The aim of the work was to prepare and carry out the first stage of the study of the aptasensor based on LC-2108 aptamer and the golden screen-printed electrodes. The study included characterization of the aptamer layer obtained at the electrode surface using electrochemical methods.

2. Experimental part

Chemically pure (C.P.) reagents were obtained from Merck, Germany (2-mercaptoethanol, phosphate buffer saline pH 7.4) and from Reachim Corp., Russia (KCl, NaOH, H₂SO₄, H₂O₂, potassium hexacyanoferrates (II) and (III)). An aptamer specific to lung cancer tumor marker (LC-2108) was provided by the research group from Krasnoyarsk State Medical University (Krasnoyarsk, Russia) [4].

Golden screen-printed electrodes (AuSPE) with the diameter of 4 mm were obtained from DropSENS, Spain. Homemade Au disc electrodes (2 mm in diameter) were obtained from golden wire with the side surface covered with the polyethylene. Electrodes were pre-treated before measurements and modification. AuSPE electrodes were ultrasonicated for 10 min in distilled water prior to pre-treatment with one of five following methods. (1) “Piranha” mixture etching: a mixture of concentrated H₂SO₄ and H₂O₂ with the ratio 3:1 was applied to the electrode surface for 5 min. (2) Electrochemical treatment (ECT) in 0.1 M NaOH by cycling the potential between -0.7 and $+0.7$ V and the subsequent potentiostatic treatment at -0.7 V for 60 s. (3) ECT in 0.1 M H₂SO₄ by the recording of 25 consistent cycles from -0.1 to $+1.2$ V. (4) ECT in phosphate buffer solution (pH 7.4) in potentiostatic mode at -0.8 V for 30 s. (5) ECT in phosphate buffer solution (pH=7.4) in potentiostatic mode at $+1.4$ V for 30 s.

Disc golden electrodes were polished with alumina slurry and rinsed with distilled water. Then disc electrodes were ultrasonicated in ethanol for 10 min. Piranha mixture was used to finish the disc electrodes pretreatment.

Electrodes modification was carried out through the standard protocol of aptamer immobilization from its solution [5]. Pretreated electrode surface was dried and covered with 1 μ M aptamer solution: 8 μ l for AuSPE and 2 μ l for Au disc electrode. Then the electrode was incubated for 24 hours at 4°C. After rinsing with MQ-water, electrode surface was covered with 2-mercaptoethanol and incubated for 30 min. Then the electrode was rinsed with ethanol, water, and after that was covered with phosphate buffer solution (PBS, pH 7.4) to prevent aptamer structure decomposition.

Electrochemical measurements were carried out using an Electrochemical Analyzer CH 660D, CH Instruments, USA. Pt wire counter electrode and Ag/AgCl reference were used with Au disc electrodes.

Cyclic voltammetry (CV) and electrochemical impedance spectroscopy (EIS) methods were used to characterize the electrodes surface. For CVs registration, potential (E) was scanned from -0.3 to $+0.7$ V with the rate of 0.05 V/s. Impedance spectra were measured with the $E_{1/2}$ (calculated from CVs) as initial potential. E amplitude was 0.005 V and frequency changed from 1 to 100,000 Hz. Potassium chloride 0.1 M solution was used as a background electrolyte, and 25 mM equimolar solution of potassium hexacyanoferrates (II) and (III) was used as a redox probe. The “real” surface area (S_{real}) of the electrodes was calculated on the basis of Randles-Shevcik equation.

3. Results and discussion

It is known, that the electrode surface pretreatment is one of the most important factors affecting the aptamer layer formation. Among the most often used methods of electrode pretreatment for aptamer immobilization, chemical etching with Piranha mixture is widely used. Piranha mixture (freshly prepared solution of sulfur acid and hydrogen peroxide in the ratio of 3:1), removes contaminants including organic impurities. However, electrochemical pretreatment methods are also used. In this work, we studied the effect of pretreatment on AuSPE surface area.

The segments of CVs for AuSPE with different pre-treatments obtained in 0.025 M equimolar solution of potassium hexacyanoferrates (II) and (III) are presented in figure 1. It is seen, that the peak shifted from 0.205 V (for PBS treatments) to 0.170 V (for Piranha pretreatment). In addition, AuSPE treated with Piranha showed better-pronounced peak shape and lower peak-to-peak separation (ΔE) between anodic (E_a) and cathodic (E_c) peaks (table 1). According to the S_{real} calculated for these electrodes (Table 1), all pretreated electrodes exhibited electroactive surface area that is greater than the geometric one (geometric surface area of AuSPE is $1.26 \cdot 10^{-1} \text{ cm}^2$). However, S_{real} for Piranha treated electrode was found to be the largest, although its difference from the electrode treated in sodium hydroxide lied within the error margin.

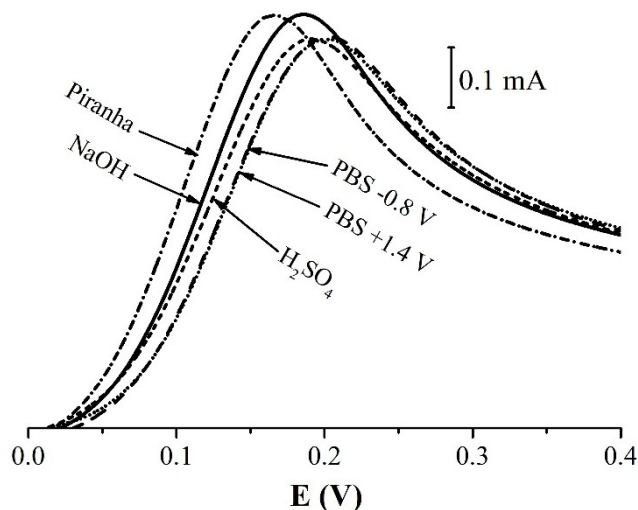


Figure 1. The peaks on CVs of anodic oxidation of $[\text{Fe}(\text{CN})_6]^{4-}$ on the surface of AuSPE pretreated with different methods.

Table 1. Calculation results for the real electroactive surface area of AuSPE after different pre-treatment.

Pre-treatment	$S_{real} (\text{cm}^2)$	$E_a (\text{V})$	$E_c (\text{V})$	$\Delta E (\text{V})$
Piranha etching	$(1.78 \pm 0.06) \cdot 10^{-1}$	0.170	0.069	0.101
ECT in NaOH	$(1.77 \pm 0.09) \cdot 10^{-1}$	0.185	0.082	0.103
ECT in H_2SO_4	$(1.75 \pm 0.04) \cdot 10^{-1}$	0.190	0.084	0.106
ECT in PBS -0.8 V	$(1.61 \pm 0.07) \cdot 10^{-1}$	0.202	0.085	0.117
ECT in PBS $+1.4 \text{ V}$	$(1.5 \pm 0.4) \cdot 10^{-1}$	0.205	0.083	0.122

Electrochemical impedance spectra for the AuSPE with different pre-treatments were measured in potassium hexacyanoferrates (II) and (III) solution as well. EIS data normally is plotted as Nyquist plot and can provide a direct information on electron transfer resistance in the system. Impedance

spectra of the electrodes are presented in figure 2. The Nyquist plot for AuSPE pre-treated with the Piranha solution (figure 2b) is more close to the widely described Randles model of the equivalent circuit (see, for example [6,7]). A linear part of the curve at the lower frequencies represents a process limited by the diffusion, and a semicircle in higher frequencies part of the spectrum belongs to the electron transfer limitation. The rest of the electrodes showed more complicated impedance behavior (shape of the semicircle parts, the tilt angle of the linear parts). Thus, based on CV and EIS results the Piranha treatment was chosen for the electrodes pre-treatment before aptamer immobilization.

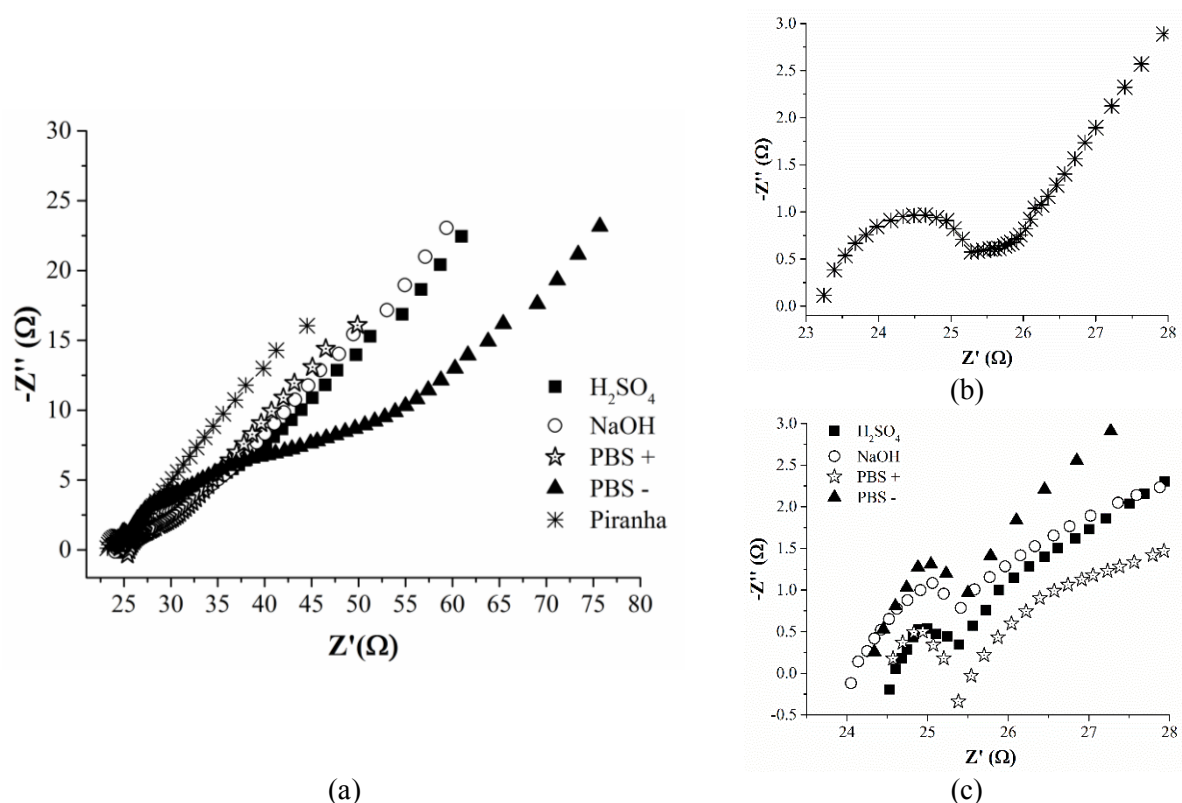


Figure 2. EIS data for the AuSPE pretreated with different methods: (a) the whole Nyquist plots; (b) the high-frequency region of the Nyquist plot for Piranha pre-treated electrode; (c) the high-frequency region of the Nyquist plot for the rest of the electrode pre-treatments.

AuSPE electrodes pre-treated with Piranha and modified with LC-2108 aptamer and MET were studied by cyclic voltammetry. Calculated S_{real} values are presented in table 2. It is seen, that electrode electroactive surface area decreases for AuSPE covered with MET. But, aptamer-modified electrode exhibited greater surface area than the bare AuSPE. The result seem to be unusual, since biomolecules presence should decrease S_{real} .

The EIS data for AuSPE modified with MET and LC-2108 aptamer presented in figure 3. There is a deviation from the supposed common scenario, where the aptamer presence increases the semicircle diameter. It is seen, that in the case under study aptamer and MET presence decreased the semicircle part diameter of the spectra R_{et} from 25.5 to 25 Ω . The tilt angle of the line changed in the initial part (figure 3b) indicating the second semicircle possible presence. This feature points at the more complicated diffusion limitations of the process when the electrode is covered with the aptamer and 2-mercaptoethanol. This may be explained by the unordinary or irregular structure of the aptamer/MET layer on the Au surface or by the specific electrochemical properties of the aptamer itself.

Table 2. Calculation results for the real electroactive surface area of AuSPE and Au disc electrodes after MET and LC-2108 immobilization.

Electrode	$S_{\text{real}} \text{ (cm}^2\text{)}$	$S_{\text{geom.}} \text{ (cm}^2\text{)}$
AuSPE	$(1.78 \pm 0.04) \cdot 10^{-1}$	
AuSPE/MET	$(1.64 \pm 0.06) \cdot 10^{-1}$	$1.26 \cdot 10^{-1}$
AuSPE/MET/LC-2108	$(1.86 \pm 0.01) \cdot 10^{-1}$	
Au disc	$(3.8 \pm 0.4) \cdot 10^{-2}$	
Au disc/MET	$(3.7 \pm 0.4) \cdot 10^{-2}$	$3.14 \cdot 10^{-2}$
Au disc/MET/LC-2108	$(3.9 \pm 0.5) \cdot 10^{-2}$	

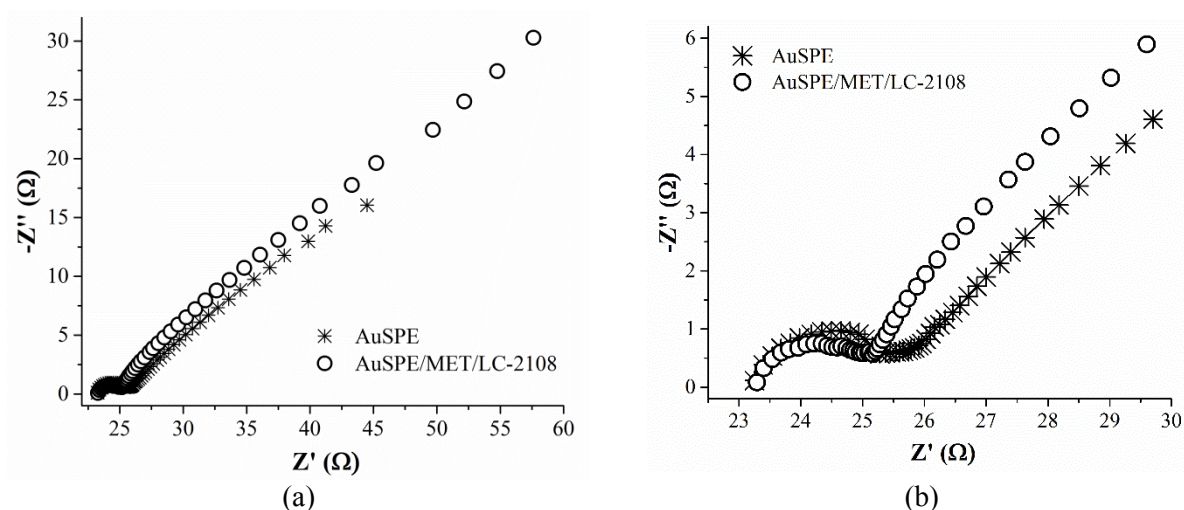


Figure 3. EIS data for bare AuSPE and AuSPE modified with LC-2108 aptamer and MET: (a) the whole Nyquist plot; (b) the high-frequency region of the Nyquist plot.

To establish whether the results obtained were influenced by the specificity of Au screen-printed electrodes (or the specific interaction of the aptamer with AuSPE electrode), we carried out the experiment with polycrystalline Au disc electrodes (2 mm in diameter). Au disc electrode was polished (alumina slurry) before ultrasonication. After that, the Piranha pre-treatment, aptamer immobilization, and MET surface blocking procedures were similar to those for AuSPE. CVs for the disc electrodes before and after aptamer immobilization, along with the control experiment with MET Au surface blocking only, are presented in figure 4.

It can be seen, that LC-2108 presence on the electrode surface led to the decrease of the peak-to-peak separation. Moreover, peaks were better pronounced. Table 2 shows S_{real} surface area of the bare and modified electrodes. So, in spite of the CVs difference, the peaks' height (S_{real} was calculated from it) did not change significantly; the change was within the measurement error. However, the tendency was similar to that for AuSPE: S_{real} decreased for MET and increased for LC-2108 modified electrodes.

To further understanding the aptamer presence influence on the electrode electrochemical signal, impedance measurements were carried out. EIS data obtained for Au disc electrodes pre-treated with Piranha solution and modified with 2-mercaptoethanol and LC-2108 aptamer is presented in figure 5. In this case, the spectra showed the similar shape, but the semicircle part differed. It is surprising that bare Au disc electrode exhibited R_{et} lower than the electrode covered with MET but higher than Au

disc/MET/LC-2108. It seems as if the aptamer presence prevented the surface blocking by MET and facilitated the electron transfer through the electrode-solution boundary.

Thus, the LC-2108 aptamer specific to tumor marker of lung cancer showed unusual electrochemical behaviour. This may be explained by the unordinary or irregular structure of the aptamer/MET layer on the Au surface or by the specific electrochemical properties of the aptamer itself. Thus, detailed study of the aptamer electrochemical properties is required.

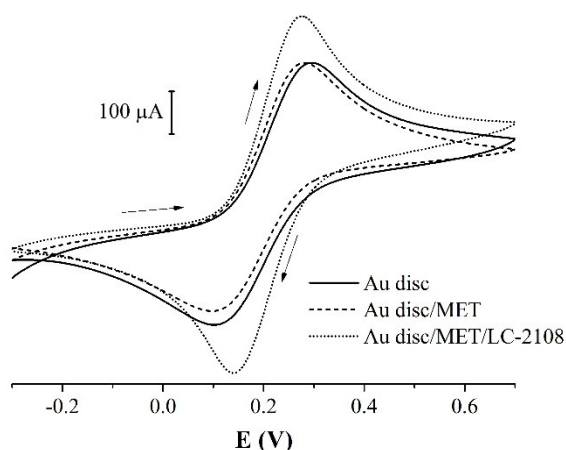


Figure 4. CVs for bare Au disc electrode and modified with LC-2108 aptamer and MET.

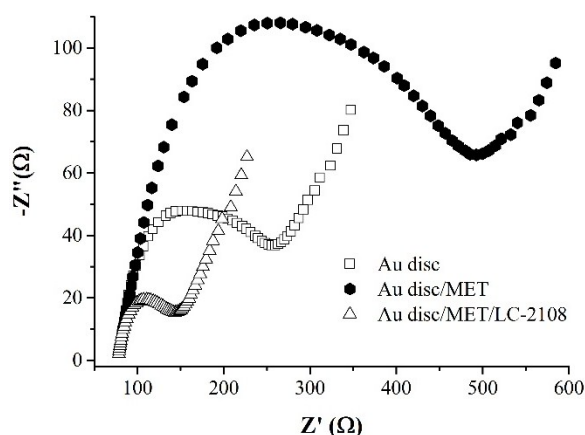


Figure 5. EIS data for bare Au disc electrode and electrode modified with LC-2108 aptamer and MET.

4. Conclusion

New-developed DNA-aptamer LC-2108 specific to lung cancer tumor marker was immobilized on the surface of golden screen-printed electrodes and Au disc electrodes. The change of electrochemical behavior of the electrodes before and after immobilization was studied.

It was shown that aptamer presence surprisingly caused the growth of the electroactive electrode surface area. Moreover, aptamer decreased the resistance of electron transfer through the electrode surface. Unusual electrochemical behavior of LC-2108 aptamer shown in the paper is controversial to the described in the literature. Thus, a detailed study of the LC-2108 aptamer electrochemical properties is required.

Acknowledgments

The work is supported by the Grant of the President of the Russian Federation (MK-5284.2018.3).

References

- [1] Arduini F, Cinti S, Scognamiglio V and Moscone D 2016 Nanomaterials in electrochemical biosensors for pesticide detection: advances and challenges in food analysis *Microchim. Acta* **183** 2063
- [2] Sefah K, Shangguan D and Xiong X 2010 Development of DNA aptamers using Cell-SELEX *Nature Protocols* **5** 1169
- [3] Rapini R and Marrazza G 2017 Electrochemical aptasensors for contaminants detection in food and environment: Recent advances *Bioelectrochem.* **118** 47
- [4] Zamay G, Kolovskaya O, Zamay T, Glazyrin Y, Krat A, Zubkova O, Spivak E, Wehbe M, Gargaun A, Muharemagic D, Komarova M, Grigorieva V, Savchenko A, Modestov A, Berezovski M and Zamay A 2015 Aptamers selected to postoperative lung adenocarcinoma detect circulating tumor cells in human blood *Mol. Ther.* **23** 1486
- [5] Zamay G, Zamay T, Kolovskii V, Shabanov A, Glazyrin Y, Veprintsev D, Krat A, Zamay S,

- Kolovskaya O, Gargaun A, Sokolov A, Modestov A, Artyukhov I, Chesnokov N, Petrova M, Berezovski M and Zamay A 2016 Electrochemical aptasensor for lung cancer-related protein detection in crude blood plasma samples *Sci. Rep.* **6** 34350
- [6] Xia N, Wang X, Yu J, Wu Y, Cheng S, Xing Y and Liu L 2017 Design of electrochemical biosensors with peptide probes as the receptors of targets and the inducers of gold nanoparticles assembly on electrode surface *Sens. Actuators B Chem.* **239** 834
- [7] Talemi RP, Mousavi SM and Afruzi H 2017 Using gold nanostars modified pencil graphite electrode as a novel substrate for design a sensitive and selective dopamine aptasensor *Mater. Sci. Eng. C* **73** 700